PHYSICAL REVIEW A VOLUME 42, NUMBER 9 1 NOVEMBER 1990

Multiconfiguration Dirac-Fock calculations of transition energies with QED corrections in three-electron ions

P. Indelicato
National Institute of Standards and Technology, Gaithersburg, Maryland 20899
and Laboratoire de Physique Atomique et Nucléaire, Université Pierre et Marie Curie, Paris, France

J. P. Desclaux
Département de Recherche Fondamentale, Service de Physique Atomique,
Centre d'Etudes Nucléaires de Grenoble, Boîte Postale No. 85X, F-38041 Grenoble CEDEX, France

(Received 18 December 1989; revised manuscript received 20 June 1990)

We present accurate calculations of the $1s^22s$ and $1s^22p$ energy levels of lithiumlike ions for $15 \leq 2Z \leq 92$. The multiconfiguration Dirac-Fock method has been used to calculate relativistic effects. One-electron radiative corrections and estimated screening corrections have been calculated. These results are in good agreement with relativistic many-body calculations. General agreement with experimental transition energies (available up to $Z=92$) is very good.

I. INTRODUCTION

With the increasing availability of very precise high-Z data for transition energies in a few-electron ions, it has become increasingly interesting to undertake fully relativistic calculations. Testing quantum electrodynamics in those systems is of particular interest since they are very often more accessible to experiments than corresponding one-electron ions. The study of bound many-electron systems in a relativistic model is still a challenge since such a problem lacks a simple exact Hamiltonian form. One has then to deal with many difficulties superimposed on the usual problem of computing correlation effects, and to take care of radiative corrections. In the past few years several works have succeeded in improving the precision of transition energies in two-electron[1-6] and three-electron ions.[5,7] In previous work we have used the multiconfiguration Dirac-Fock (MCDF) method for computing transition energies in two-electron ions. We have also proposed a semiclassical approximation for the two-electron self-energy correction (screening of the self-energy). These two method together have produced results in good agreement with all available experimental values for $10 \leq Z \leq 92$, for both $2p$-$1s$ and $2p$-$2s$ transitions. In this paper we have extended those calculations to the three lowest levels of lithiumlike ions with $15 \leq Z \leq 92$. We devote the second section of this paper to a description of the calculation. In the third section we compare our results with the relativistic many-body perturbation theory (RMBPT) of Refs. 6 and 7. In the fourth, we compare them with experimental values. The fifth section is our conclusion.

II. DESCRIPTION OF THE CALCULATION

A. Uncorrelated energy

The MCDF method[8,9] is the relativistic equivalent of the multiconfiguration Hartree-Fock method (MCHF)—see, for example, Ref. 10—the wave function being expanded as a sum of Slater determinants of four-component Dirac spinors. Our effective Hamiltonian is identical with the one discussed in Ref. 2. The nucleus is represented by a Fermi distribution of the nuclear charge. All calculations were done using experimental values for the nuclear radius, when available, and a semiempirical formula[11] otherwise. The effective electron-electron interaction operator is based on the one-photon exchange approximation, deduced from the Feynman diagram in Fig. 1(a). This operator is gauge dependent, and in a nonlocal approximation like the MCDF method, the contribution to the energy is also gauge dependent.[12] It has been shown theoretically,[13-15] and confirmed by comparison with experimental data in two-electron systems,[16] that the Coulomb gauge must be used to avoid the appearance of a spurious contribution in the one-photon exchange approximation. Here we will distinguish the usual three parts in the electron-electron interaction, i.e, the Coulomb, magnetic, and retardation interactions. The three corresponding diagrams are represented in Figs. 1(b), 1(c), and 1(d), respectively. The expression for the operator representing the interaction between electrons i and j in the Coulomb gauge is

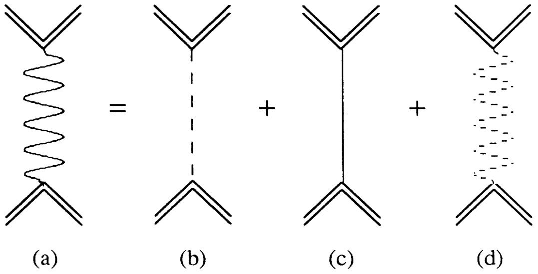

FIG. 1. Feynman diagrams for the electron-electron interaction.

$$g_{ij}=g_{ij}^{\mathrm{Coul}}+g_{ij}^{\mathrm{Mag}}+g_{ij}^{\mathrm{Ret}}\ , \tag{1a}$$

$$g_{ij}^{\mathrm{Coul}}=\frac{1}{r_{ij}}\ , \tag{1b}$$

$$g_{ij}^{\mathrm{Mag}}=\frac{-\boldsymbol{\alpha}_1\cdot\boldsymbol{\alpha}_2}{r_{ij}}\ , \tag{1c}$$

$$g_{ij}^{\mathrm{Ret}}=\left[-\boldsymbol{\alpha}_1\cdot\boldsymbol{\alpha}_2\frac{\cos(\omega_{ij}r_{ij})-1}{r_{ij}}+(\boldsymbol{\alpha}_1\cdot\boldsymbol{\partial}_1)(\boldsymbol{\alpha}_2\cdot\boldsymbol{\partial}_2)\frac{\cos(\omega_{ij}r_{ij})-1}{\omega_{ij}^2 r_{ij}}\right]\ , \tag{1d}$$

where ω_{ij} is the energy of the photon exchanged between the two electrons, r_{ij} is the interelectronic distance, and $\boldsymbol{\alpha}_i$ are the Dirac matrices. The operators g_{ij}^{Coul}, g_{ij}^{Mag}, and g_{ij}^{Ret} are, respectively, the Coulomb, magnetic, and retardation operators.

Our zeroth-order energy is computed using the Coulomb operator and a single configuration in the expansion of the wave function, leading to the Coulomb contribution. The resulting single-configuration wave function is used to obtain the magnetic contribution and the retarded contribution in first order.

For completeness, we have used the reduced Rydberg constant for all states, and corrected the $2p$ states for mass polarization, using the Hughes-Eckhart[17] formula. The values of the fundamental constants are those of the 1986 adjustment.[18] To convert our values from eV to Å one should use $C=12\,398.4244$ eV Å, and to cm^{-1}, $C'=8065.5410\ \mathrm{cm}^{-1}/\mathrm{eV}$. The fine-structure constant is taken to be $\alpha=1/137.0359\,895$ and the conversion from atomic unit to eV is done using 1 hartree$=27.2113\,961$ eV.

B. Electron correlation

To get accurate values of the energy, it is mandatory to go beyond the one-particle approximation presented in Sec. II A. Following the method described in Ref. 2, we have computed the energies of $1s^22s$ and $1s^22p$ levels in lithiumlike ions, including all significant configurations involving the $n=3$ shell for both core and outer electrons. To get the best result we did all our calculation in the optimized level (OL) scheme where the radial wave functions are optimized separately for each level. The three-electron problem in the relativistic case is much more complicated than the two-electron one. The number of jj configurations to get reasonable precision is far larger (53 for the $1s^22p_{3/2}$, see Table I) than for heliumlike systems (9 for $1s^2$), and one has to be careful in the evaluation of the $2p_{1/2}$-$2p_{3/2}$ fine-structure splitting. In nonrelativistic calculations both levels will have the same correlation energy. In relativistic MCDF calculations, since the $2p_{1/2}$ and $2p_{3/2}$ radial wave functions are adjusted independently in the self-consistent process, and because of the different possible couplings for certain configurations such as $2p^3$, the correlation energies need not be the same for $J=\frac{1}{2}$ and $\frac{3}{2}$ in the nonrelativistic limit.[19] This will remain true even for a calculation with an infinite basis set. This spurious contribution to the fine-structure splitting is computed by taking the limit $\alpha=0$ in the MCDF code. The nonzero value obtained in this limit is then subtracted from the MCDF value.

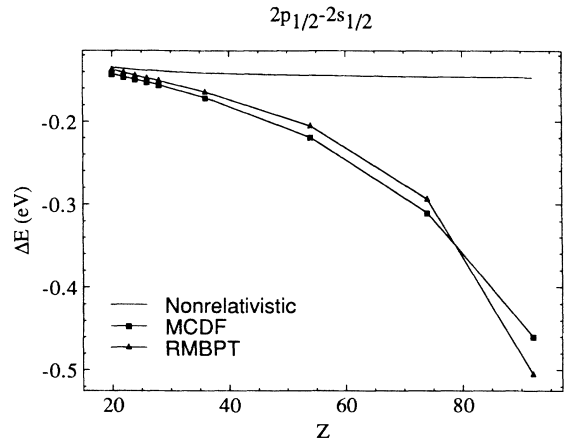

FIG. 2. Comparison between nonrelativistic electrostatic correlation energies, MCDF correlation, and RMBPT correlation (Ref. 7) for the $2p_{1/2}$-$2s$ transition.

To compensate for the finite number of configurations in our basis set we proceed as follows: As the correlation energies can be expanded in a double series in $1/Z$ and $Z\alpha$,[20] and the nonrelativistic (NR) correlation energy can be written as

$$\Delta E_{\mathrm{corr}}^{\mathrm{NR}}=\Delta E_0+\Delta E_1\frac{1}{Z}+\Delta E_2\frac{1}{Z^2}+\Delta E_3\frac{1}{Z^3}+\cdots\ , \tag{2}$$

we have used the exact nonrelativistic calculation of Horak *et al.*[21] for the ΔE_0 term and fitted the much smaller contribution of the higher-order terms to the nonrelativistic limit of our MCDF calculation (i.e., the one with the fine-structure constant set to 0). Our final correlation correction to the level energy is then this nonrelativistic correlation energy and the relativistic one defined by $\Delta E_{\mathrm{Corr}}^{\mathrm{MCDF}}-\Delta E_{\mathrm{Corr}}^{\mathrm{MCHF}}$ where MCHF refers to the nonrelativistic limit of MCDF. The resulting electrostatic correlation energies for the $2p_{1/2}$-$2s$, $2p_{3/2}$-$2s$, and $2p_{3/2}$-$2p_{1/2}$ transitions are plotted in Figs. 2–4 and com-

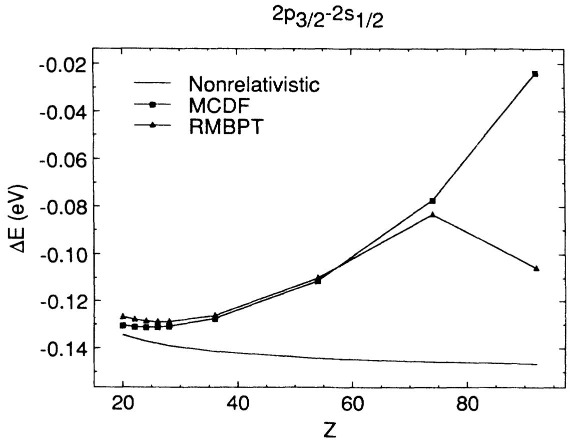

FIG. 3. Comparison between nonrelativistic electrostatic correlation energies, MCDF correlation, and RMBPT correlation (Ref. 7) for $2p_{3/2}$-$2s$ transition.

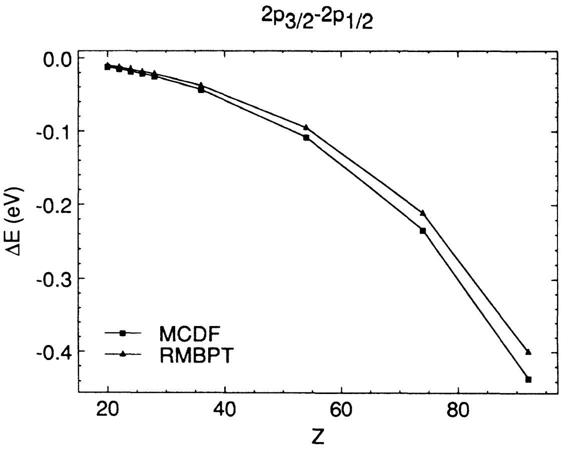

FIG. 4. Comparison between MCDF and RMBPT (Ref. 7) correlation energies for $2p_{3/2}$-$2p_{1/2}$ splitting.

pared with results from Ref. 7. As in the heliumlike case for which the relativistic contribution to electrostatic correlation energy was maximum for the $1s2p\ ^3P_0$ level, the $1s^22p_{1/2}$ level is most affected in lithiumlike ions because of the s character of the small component of the $p_{1/2}$ orbital.

An even more delicate task is to account for many-body effects in the magnetic and retarded interaction. As pointed out by several authors (see, for example, Refs. 2, 22, and 23), it is probably legitimate to include the magnetic operator in the self-consistent-field (SCF) process to get a more accurate magnetic contribution. However, this was shown only for single-configuration calculations. In this work we did not perform such a calculation for all Z, because of serious problems in reaching convergence for this operator with large basis sets at high Z. It would have also required an unacceptable amount of computer time, because of the large number of magnetic integrals involved in the calculation (about 10 times more than Coulomb integrals).

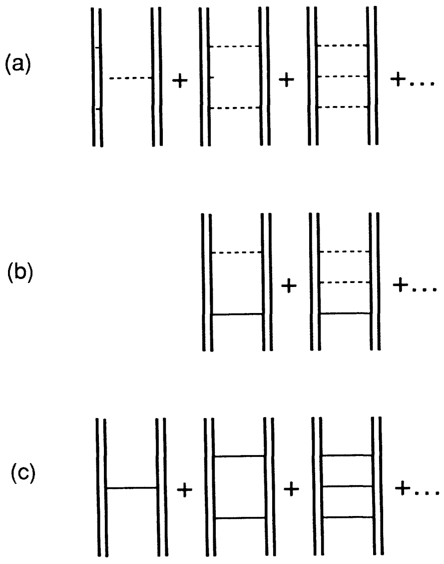

FIG. 5. Feynman diagrams for the ladder approximation.

Expanding the basis set with the Coulomb interaction in the SCF process amounts to including more and more of the Coulomb "ladder approximation" diagrams in the calculation. The diagrams corresponding to the ladder approximation draw their name from their characteristic shape [Fig. 5(a)]. If we could do the same calculation with the magnetic interaction in the SCF process, that would include the ladder approximation with all combinations of several instantaneous Coulomb and transverse photons [Figs. 5(b) and 5(c)]. A more limited approximation we have used consists in using the (pure Coulomb) MCDF wave functions to compute the expectation value of the magnetic operator [Eq. 1(c)]. Here we are only including diagrams in which there is one instantaneous transverse photon and any number (within our basis-set size) of Coulomb photons [Fig. 5(b)]. This is the leading effect, and higher-order effects will show up only

TABLE I. List of the configurations included in the calculation of the correlation energy.

Configurations for the $1s^22s$ level (LS)	Number of jj configurations	Configurations for the $1s^22p_{1/2}$ level (LS)	Number of jj configurations	Configurations for the $1s^22p_{3/2}$ level (LS)	Number of jj configurations
$1s^22s$	1	$1s^22p$	1	$1s^22p$	1
$2s2p^2$	3	$2p^3$	1	$2p^3$	3
$2s3s^2$	1	$2p2s^2$	1	$2p2s^2$	1
$1s2p^2$	3	$2p3s^2$	1	$2p3s^2$	1
$1s2s3s$	2	$2p3p^2$	6	$2p3p^2$	8
$2s^23s$	1	$2p^23p$	6	$2p^23p$	8
$1s2p3p$	6	$1s2p2s$	3	$1s2p2s$	3
$2s3p^2$	3	$1s2s3p$	3	$1s2s3p$	3
$2s3d^2$	3	$1s2p3d$	4	$1s2p3d$	7
$1s3s^2$	1	$2p3d^2$	7	$2p3d^2$	11
$1s3p^2$	3	$1s3p3d$	4	$1s3p3d$	7
$1s3p^2$	3				
Total number (jj)	30		37		53

for the highest Z. Using a restricted number of configurations with the magnetic interaction in the SCF process we can estimate the order of magnitude of these contributions to be of a few tenths of an eV for $Z=92$.

The case of the retarded interaction is even more intricate. Equation (1d) is a compact reduction of a complex operator[14] involving exponential functions of the one-electron Hamiltonian. This compact reduction can be performed only if single-electron energies can be defined as for the independent-particle approximation or for Hartree-Fock wave functions with the help of the Koopman's theorem. To compute many-body effects the full operator should be used, a difficult task that has not yet been done. Thus to obtain an order of magnitude of the uncertainty arising from the neglect of many-body effects we have nevertheless used Eq. (1d) with the ω_{ij} defined with the help of diagonal Lagrange multipliers (i.e., the Lagrange parameters introduced to ensure normalization of the one-electron orbitals).

C. QED corrections

Once the correlation is taken into account, one has to include radiative corrections. Vacuum polarization potentials of order $\alpha(Z\alpha)$ (Uehling contribution), $\alpha^2(Z\alpha)$ (Källén and Sabry contribution), and $\alpha(Z\alpha)^3$ are used to provide screened vacuum polarization corrections. The Feynman diagrams corresponding to these three potentials are represented in Fig. 6. The Uehling potential arises from the diagram with one interaction with the nuclear potential, the $\alpha(Z\alpha)^3$ potential has three interactions with the nuclear potential. They represent the two lowest orders of the expansion in power of $Z\alpha$ of the first-order vacuum polarization (Fig. 6, top). The Källén and Sabry potential (Fig. 6, bottom) is the leading term of the diagrams of order α^2. These corrections are evaluated using first-order perturbation theory with Dirac-Fock wave functions. The use of Dirac-Fock wave functions rather than hydrogenic ones should account for most of the screening of the vacuum polarization, and it also takes care of the finite-nuclear-size correction by using the correct expressions for the Uehling and Källén and Sabry potential.[24] For very high Z the modification of the Uehling potential due to the presence of other electrons could play a significant role and should be investigated further.

Unfortunately there is no potential for the self-energy correction and one has to find other ways to estimate the self-energy screening. In this calculation we have included the hydrogenic self-energy[25–27] corrected for finite nuclear size.[11] The approximation for self-energy screening described in Ref. 3 has been extended to the three-electron case. This method used an effective potential to correct the lowest-order part in $Z\alpha$ of the one-electron self-energy for two-electron effects, by correcting for the changes in the electronic density at the nucleus. This potential can be derived for example, by using Welton's semiclassical arguments. It has been shown by Dupont-Roc, Fabre, and Cohen-Tannoudji[28] that for *self-energy*, the effective Hamiltonian provided by Welton semiclassical arguments gives the proper nonrelativistic limit. Very recently Feldman and Fulton[29] have derived this effective potential by considering low-order diagrams derived from QED. While such a justification increases the interest of this method, it remains that only the lowest-order term in $Z\alpha$ is taken into account and that higher-order terms may have a sizable contribution for high-Z-like uranium.

For s electrons this method leads to a screening correction

$$\delta E_{\rm SE}^{ns}=\frac{\langle ns|\Delta U_N|ns\rangle_{\rm DF}}{\langle ns|\Delta U_N|ns\rangle_{\rm hyd}}E_{{\rm SE},ns}^{\rm hyd}\,, \tag{3}$$

where the subscripts DF and hyd stand for Dirac-Fock or hydrogenlike wave functions, respectively, U_N is the nuclear potential, and $E_{{\rm SE},ns}^{\rm hyd}$ the one-particle self-energy from Refs. 25–27 corrected for finite-nuclear size effects.[11] For $p,d,\ldots,$ electrons, the above correction, which is proportional to the square of the wave function at the origin cancels, and the $g-2$ (also called vertex correction) diagram provides the leading screening correction

$$\delta E_{\rm SE}^{nl\geq 3}=\frac{\langle nl\geq 3|\beta\boldsymbol{\alpha}\cdot\mathbf{E}|nl\geq 3\rangle_{\rm DF}}{\langle nl\geq 3|\beta\boldsymbol{\alpha}\cdot\mathbf{E}|nl\geq 3\rangle_{\rm hyd}}E_{{\rm SE},nl\geq 3}^{\rm hyd}\,, \tag{4}$$

where E is the nuclear electric field.

One also can get a mean-field estimate for the self-energy correction to the electron-electron interaction by replacing U_N by the Dirac-Fock potential in Eq. (3).[3] Yet one has to be careful that only pairs of electrons in singlet states contribute to the self-energy correction to the electron-electron interaction. Therefore we have expanded the three-electron Slater determinant as the sum of three two-electron determinants multiplied by a one-electron wave function and have kept only singlet terms in the sum.

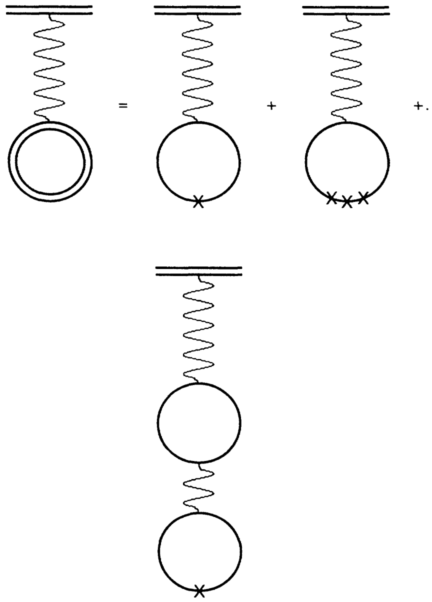

FIG. 6. Feynman diagrams for the vacuum polarization. X represents interaction with the nucleus. Top: first-order vacuum polarization and its expansion in powers of $Z\alpha$, i.e., in number of interactions with the nucleus. Bottom: first order in $Z\alpha$ of the second-order vacuum polarization (Källén and Sabry contribution).

TABLE II. Contributions to the $1s^22s$ energy for $Z=15,54,92$ in units of eV. Each individual contribution is corrected for finite nuclear size. Number of decimal figures corresponds to numerical accuracy only.

Z	15	54	92
Coulomb	-6499.455	$-91\,536.069$	$-295\,163.435$
Magnetic	1.256	65.254	368.581
Retardation (order ω^2)	-0.012	-0.756	-4.915
Higher-order retardation ($>\omega^2$)	0.000	0.048	0.645
Mass polarization	0.000	0.000	0.000
Electrostatic correlation (NR)	-1.429	-1.451	-1.454
Electrostatic correlation (Rel)	-0.001	-0.026	-0.239
Magnetic correlation	-0.087	-1.245	-3.601
Hydrogenlike self-energy	1.382	109.683	771.570
Self-energy screening	-0.077	-1.971	-10.757
Self-energy screening ($e^- - e^-$)	-0.003	-0.034	-0.063
Vacuum polarization [Uehling, $\alpha(Z\alpha)$]	-0.084	-15.423	-202.073
Vacuum polarization $\alpha(Z\alpha)^3$	0.000	0.346	9.815
Vacuum polarization [Källén and Sabry, $\alpha^2(Z\alpha)$]	-0.001	-0.122	-1.547
Total energy	-6498.510	$-91\,381.765$	$-294\,237.473$
Retardation correlation	0.021	0.317	1.115

D. Results

The results obtained in the three preceding subsections are shown in Tables II–VII. In Tables II–V we present individual values of terms described previously for $Z=15$, 54, and 92 to show their relative variations. The successive entries are, respectively, the following.

(i) Coulomb: the single configuration eigenvalue of the Dirac-Fock equation with the Coulomb operator, Eq. (1b) for the electron-electron interaction as described in Sec. II B.

(ii) Magnetic: the contribution of the magnetic operator, Eq. (1c) in the first order of perturbation, as described in Sec. II A.

(iii) Retardation (order ω^2): the retardation contribution in first order, limited to the ω^2 term in the expansion of the cosine in Eq. (1d).

(iv) Higher-order retardation ($>\omega^2$): the remaining terms in the expansion of the cosine in Eq. (1d).

(v) Mass polarization: the mass polarization as described in Sec. II A.

TABLE III. Contributions to the $1s^22p\ J=\frac{1}{2}$ energy for $Z=15,54,92$ in units of eV. Each individual contribution is corrected for finite nuclear size. Number of decimal figures corresponds to numerical accuracy only.

Z	15	54	92
Coulomb	-6473.524	$-91\,415.397$	$-294\,876.002$
Magnetic	1.358	72.295	410.555
Retardation (order ω^2)	-0.034	-2.010	-10.096
Higher-order retardation ($>\omega^2$)	0.000	-0.031	0.288
Mass polarization	-0.006	-0.024	-0.039
Electrostatic correlation (NR)	-1.558	-1.595	-1.601
Electrostatic correlation (Rel)	-0.005	-0.101	-0.552
Magnetic correlation	-0.086	-1.179	-3.289
Hydrogenlike self-energy	1.293	102.049	715.856
Self-energy screening	-0.060	-1.551	-9.007
Self-energy screening ($e^- - e^-$)	-0.002	-0.032	-0.059
Vacuum polarization [Uehling, $\alpha(Z\alpha)$]	-0.079	-14.497	-188.764
Vacuum polarization $\alpha(Z\alpha)^3$	0.000	0.327	9.252
Vacuum polarization [Källén and Sabry, $\alpha^2(Z\alpha)$]	-0.001	-0.115	-1.447
Total energy	-6472.704	$-91\,261.863$	$-293\,954.905$
Retardation correlation	0.022	0.324	1.038

TABLE IV. Contributions to the $1s^22p$ $J=\frac{3}{2}$ energy for $Z=15,54,92$ in units of eV. Each individual contribution is corrected for finite nuclear size. Number of decimal figures corresponds to numerical accuracy only.

Z	15	54	92
Coulomb	−6472.045	−91 036.827	−290 647.640
Magnetic	1.262	65.726	364.664
Retardation (order ω^2)	−0.034	−2.017	−10.258
Higher-order retardation ($>\omega^2$)	−0.001	−0.432	−6.344
Mass polarization	−0.006	−0.024	−0.039
Electrostatic correlation (NR)	−1.558	−1.595	−1.601
Electrostatic correlation (Rel)	0.001	0.007	−0.117
Magnetic correlation	−0.086	−1.237	−3.596
Hydrogenlike self-energy	1.298	102.702	715.293
Self-energy screening	−0.062	−1.577	−8.306
Self-energy screening ($e^- - e^-$)	−0.002	−0.032	−0.056
Vacuum polarization [Uehling, $\alpha(Z\alpha)$]	−0.079	−14.462	−186.342
Vacuum polarization $\alpha(Z\alpha)^3$	0.000	0.326	9.105
Vacuum polarization [Källén and Sabry, $\alpha^2(Z\alpha)$]	−0.001	−0.115	−1.428
Total energy	−6471.313	−90 889.557	−298 776.663
Retardation correlation	0.020	0.323	1.113

TABLE V: Total energy for the $1s^22s$ level with main contributions (eV): Coulomb includes mass polarization, Breit is the sum of the magnetic and retarded contributions, Corr is the sum of electrostatic and magnetic correlation energies, and QED is the sum of one-particle self-energy, self-energy screening, and the three contributions to vacuum polarization. Number of decimal figures corresponds to numerical accuracy only.

Z	Coulomb	Breit	Corr.	QED	Total
15	−6499.455	1.244	−1.517	1.218	−6498.510
16	−7426.492	1.518	−1.532	1.526	−7424.980
17	−8416.016	1.830	−1.547	1.884	−8313.849
18	−9468.193	2.183	−1.563	2.297	−9465.277
19	−10 583.176	2.578	−1.580	2.768	−10 579.410
20	−11 761.182	3.018	−1.597	3.303	−11 756.458
22	−14 307.084	4.045	−1.634	4.579	−14 300.095
24	−17 107.621	5.284	−1.675	6.159	−17 097.852
26	−20 164.750	6.755	−1.718	8.080	−20 151.633
28	−23 480.627	8.481	−1.765	10.377	−23 463.535
29	−25 236.332	9.446	−1.790	11.678	−25 216.999
30	−27 057.616	10.482	−1.816	13.087	−27 035.862
32	−30 898.300	12.781	−1.871	16.249	−30 871.141
34	−35 005.465	15.399	−1.929	19.900	−34 972.094
36	−39 382.151	18.361	−1.991	24.079	−39 341.702
40	−48 957.532	25.407	−2.126	34.184	−48 900.066
42	−54 163.534	29.541	−2.199	40.194	−54 095.998
45	−62 506.979	36.576	−2.316	50.526	−62 422.193
47	−68 432.134	41.861	−2.400	58.361	−68 334.312
50	−77 876.352	50.749	−2.532	71.645	−77 756.489
54	−91 536.069	64.547	−2.722	92.479	−91 381.765
60	−114 415.077	89.923	−3.037	131.300	−114 196.891
65	−135 796.011	115.946	−3.325	171.610	−135 511.779
70	−159 427.722	147.047	−3.635	220.281	−159 064.028
74	−180 063.053	176.041	−3.897	266.019	−179 624.889
75	−185 475.485	183.915	−3.965	278.498	−185 017.037
80	−214 138.007	227.345	−4.316	347.562	−213 567.416
82	−226 388.507	246.761	−4.464	378.560	−225 767.651
83	−232 690.036	256.937	−4.540	394.822	−232 042.817
85	−245 658.477	278.274	−4.696	428.962	−244 955.938
90	−280 331.304	337.800	−5.115	524.388	−279 474.231
92	−295 163.435	364.312	−5.295	566.945	−294 237.473

TABLE VI. Total energy for the $1s^22p\ J=\frac{1}{2}$ level with main contributions (eV): Coulomb includes mass polarization, Breit is the sum of the magnetic and retarded contributions, Corr. is the sum of electrostatic and magnetic correlation energies, and QED is the sum of one-particle self-energy, self-energy screening, and the three contributions to vacuum polarization. Number of decimal figures corresponds to numerical accuracy only.

Z	Coulomb	Breit	Corr.	QED	Total
15	−6473.530	1.324	−1.649	1.151	−6472.704
16	−7398.560	1.619	−1.665	1.440	−7397.166
17	−8386.066	1.955	−1.682	1.777	−8384.016
18	−9436.214	2.334	−1.700	2.165	−9433.414
19	−10 549.157	2.760	−1.718	2.608	−10 545.507
20	−11 725.109	3.236	−1.737	3.109	−11 720.501
22	−14 266.862	4.345	−1.776	4.306	−14 259.987
24	−17 063.187	5.685	−1.819	5.787	−17 053.533
26	−20 116.036	7.279	−1.865	7.585	−20 103.036
28	−23 427.555	9.150	−1.914	9.734	−23 410.585
29	−25 181.049	10.196	−1.940	10.951	−25 161.842
30	−27 000.100	11.321	−1.967	12.252	−26 978.495
32	−30 836.249	13.817	−2.023	15.222	−30 809.233
34	−34 938.777	16.662	−2.083	18.631	−34 905.566
36	−39 310.718	19.882	−2.146	22.531	−39 270.451
40	−48 876.242	27.550	−2.283	31.953	−48 819.022
42	−54 077.117	32.052	−2.357	37.553	−54 009.869
45	−62 412.591	39.719	−2.474	47.173	−62 328.174
47	−68 332.229	45.482	−2.557	54.464	−68 234.840
50	−77 767.844	55.182	−2.688	66.819	−77 648.531
54	−91 415.421	70.253	−2.875	86.180	−91 261.863
60	−114 274.535	98.010	−3.183	122.223	−114 057.485
65	−135 637.185	126.522	−3.462	159.615	−135 354.511
70	−159 248.823	160.654	−3.765	204.734	−158 887.200
74	−179 866.741	192.529	−4.024	247.115	−179 431.121
75	−185 274.570	201.193	−4.091	258.675	−184 818.794
80	−213 913.150	249.053	−4.445	322.645	−213 345.896
82	−226 153.519	270.486	−4.595	351.351	−225 536.277
83	−232 449.920	281.729	−4.672	366.411	−231 806.452
85	−245 407.958	305.322	−4.831	398.025	−244 709.442
90	−280 054.352	371.294	−5.257	486.405	−279 201.911
92	−294 876.041	400.747	−5.442	525.831	−293 954.905

(vi) Electrostatic correlation (NR): the corrected MCHF electrostatic correlation energy from Eq. (2).

(vii) Electrostatic correlation (Rel): the difference $\Delta E_{\mathrm{Corr}}^{\mathrm{MCDF}}-\Delta E_{\mathrm{Corr}}^{\mathrm{MCHF}}$ as described in Sec. II B.

(viii) Magnetic correlation: the difference of the mean value of the magnetic operator, Eq. (1c) with correlated or uncorrelated Coulomb wave functions.

(ix) Hydrogenlike self-energy: the one-electron self-energy from Refs. 25–27 corrected for finite nuclear size.

(x) Self-energy screening: the sum of the screening contributions from Eqs. (3) and (4).

(xi) Self-energy screening ($e^- - e^-$): the self-energy correction to the electron-electron interaction as described in Sec. II C.

(xii) Vacuum polarization [Uehling, $\alpha(Z\alpha)$]: the mean value of the Uehling potential, corrected for finite nuclear size, with Dirac-Fock wave function.

(xiii) Vacuum polarization $\alpha(Z\alpha)^3$: the mean value of the Wichmann and Kroll potential,[30] with Dirac-Fock wave function.

(xiv) Vacuum polarization [Källén and Sabry, $\alpha^2(Z\alpha)$]: the mean value of the Källén and Sabry potential with Dirac-Fock wave function.

(xv) Total transition energy: the sum of all the previous contributions.

(xvi) Retardation correlation: the contribution to the uncertainty in the calculation resulting from the neglect of many-body effects on the retarded operator.

Our calculations of the three vacuum polarization contributions (xii)–(xiv) have been checked by computing hydrogenlike values with finite nucleus for several values of the atomic number Z and comparing them to values from Refs. 11 and 31.

In Tables V–VII we present values of the total level energy for $1s^22s$, $1s^22p_{1/2}$, and $1s^22p_{3/2}$, for all Z for which we have performed calculations. In these tables the first column (Coulomb) is the sum of contributions (i) and (v), the second (Breit) is the sum of contributions (ii), (iii), and (iv), the third is the sum of all correlation contributions (vi), (vii), and (viii), the fourth is the sum of all QED contributions (ix)–(xiv) and the last one (total) is

TABLE VII. Total energy for the $1s^2 2p\ J=\frac{3}{2}$ level with main contributions (eV): Coulomb includes mass polarization, Breit is the sum of the magnetic and retarded contributions, Corr. is the sum of electrostatic and magnetic correlation energies, and QED is the sum of one-particle self-energy, self-energy screening and, the three contributions to vacuum polarization. Number of decimal figures corresponds to numerical accuracy only.

Z	Coulomb	Breit	Corr.	QED	Total
15	−6472.051	1.227	−1.643	1.154	−6471.313
16	−7396.585	1.498	−1.658	1.445	−7395.300
17	−8383.478	1.807	−1.674	1.783	−8381.563
18	−9432.881	2.155	−1.691	2.172	−9430.245
19	−10 544.929	2.546	−1.708	2.617	−10 541.474
20	−11 719.815	2.981	−1.725	3.122	−11 715.437
22	−14 258.841	3.996	−1.763	4.325	−14 252.283
24	−17 051.494	5.220	−1.803	5.814	−17 042.263
26	−20 099.523	6.673	−1.846	7.623	−20 087.073
28	−23 404.851	8.377	−1.893	9.786	−23 388.581
29	−25 154.658	9.329	−1.917	11.010	−25 136.236
30	−26 969.585	10.351	−1.943	12.336	−26 948.840
32	−30 796.029	12.617	−1.996	15.310	−30 770.098
34	−34 886.665	15.197	−2.053	18.743	−34 854.777
36	−39 244.198	18.112	−2.113	22.671	−39 205.528
40	−48 771.922	25.037	−2.245	32.165	−48 716.965
42	−53 948.604	29.093	−2.317	37.809	−53 884.018
45	−62 239.922	35.986	−2.431	47.508	−62 158.860
47	−68 124.152	41.156	−2.512	54.858	−68 030.650
50	−77 496.335	49.836	−2.641	67.317	−77 381.823
54	−91 036.851	63.276	−2.825	86.842	−90 889.557
60	−113 675.647	87.894	−3.129	123.185	−113 467.696
65	−134 785.401	113.017	−3.406	160.875	−134 514.914
70	−158 063.940	142.896	−3.706	206.324	−157 718.427
74	−178 344.363	170.620	−3.963	248.976	−177 928.730
75	−183 656.414	178.127	−4.029	260.603	−183 221.713
80	−211 736.830	219.392	−4.376	324.883	−211 196.931
82	−223 712.285	237.762	−4.521	353.690	−223 125.354
83	−229 866.201	247.371	−4.595	368.795	−229 254.630
85	−242 517.634	267.481	−4.747	400.482	−241 854.418
90	−276 255.049	323.316	−5.146	488.903	−275 447.976
92	−290 647.679	348.063	−5.314	528.267	−289 776.663

the total level energy. All values in Tables II–VII are computed using nuclear radii from Ref. 11.

E. Error estimates

We shall not discuss in this section the numerical accuracy of the MCDF method that is easy to keep under control by varying self-consistency criteria, mesh size, and so on. This numerical error amounts to less than 0.003 eV for all the results presented here. The main source of uncertainty arises from the truncation in the basis-set expansion and is much more difficult to assess. In a recent paper Parpia and Grant[32] proposed a new method to extrapolate the MCDF calculation for the $1s^2$ level of heliumlike ions to infinite basis sets. This method also provides error estimates. Yet their method is difficult to generalize to three-electron systems. In the heliumlike ground-state case, each new orbital contributes only to one configuration, while in the lithiumlike case each new orbital contributes to several kinds of configurations, i.e., to different kinds of correlation. Besides, one needs to have several orbitals of the same symmetry to extrapolate to higher principal quantum number n. That means that one must have already all orbitals up to $n=6$ converged, to extrapolate meaningfully d, f, and g orbital contributions. Achieving convergence for the two-electron system in the optimized level mode for the $n=4$ shell, as in Ref. 32, is very difficult. In the three-electron case we would not reach convergence with an orbital of $n>3$.

We then used a different approach. Since Lindgren[33] (using the pair-equation technique) was able to compute results equivalent to an infinite basis MCHF calculation for $Z=3$, we compared our MCHF results from Eq. (2) with Lindgren's ones, to get an overestimate of the error by assuming that it can be reduced to the inaccuracy in the ΔE_1 coefficient only. We get an error estimate for the nonrelativistic contribution to electrostatic correlation of $0.232/Z$ eV for the ground state and of $0.325/Z$ eV for the two first excited states, resulting in an uncertainty of $0.093/Z$ eV for the transition energies.

For most heavy elements one of the main sources of uncertainly is due to uncertainty in the nuclear radius. The uncertainties listed in Ref. 11 for the finite-nuclear-size correction provide good estimates for this uncertainty. We do not have at this time a procedure to estimate uncertainty due to uncalculated terms or due to the use of a finite basis set on relativistic and magnetic correlations. From extrapolation of the results we have at low Z (see Sec. II B) with self-consistent magnetic interaction, we can conclude that for $Z=92$ we should have an uncertainty of 0.5 eV on the $2p_{1/2}$-$2s$ transition. The uncalculated many-body effects on the retarded interaction contribute by 0.1 eV to this uncertainty (see last line of Tables II–III).

From a comparison between theory and experiment for $Z \leq 54$, in two- and three-electron systems we have found our screening correction to the self-energy to be accurate to within 10%. This should lead to a 20% accuracy (0.3 eV) around $Z=92$ where higher-order terms account for up to 50% of the self-energy.

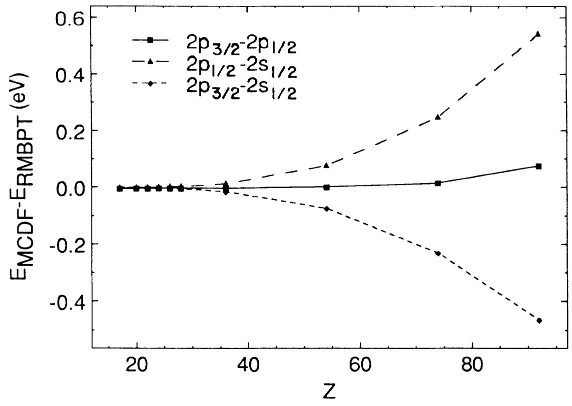

FIG. 7. Comparison between MCDF total energy (without radiative corrections) and RMBPT total energies for $2p_{1/2}$-$2s$ transition, $2p_{3/2}$-$2s$ transition, and $2p_{3/2}$-$2p_{1/2}$ splitting.

III. COMPARISON OF THEORETICAL RESULTS

Comparison of our results with those of Ref. 7 can be made in detail. But we must rely on differences between level energies, since the contributions listed in Ref. 7 are relative to a common $1s^2$ core, while our MCDF calculation gives the absolute level energy. The energy as described in Ref. 7 is obtained by the relativistic many-body perturbation theory (RMBPT). Using Ref. 7 notation, the RMBPT total energy is a sum $E=(E_0+E_1+E_2+E_3+\cdots)+(B_1+B_2+\cdots)$ where $E_0$is the Dirac-Fock Coulomb energy with a frozen core; E_1, the first-order correlation, is strictly 0; and B_i is the Breit contribution to the ith order. In this context the electrostatic correlation will be $(E_0+E_1+E_2+E_3-E_{\text{DF}})$ and the magnetic correlation (including retardation) will be $(B_1+B_2-B_{\text{DF}})$, DF denoting self-configuration Dirac-Fock energies. The comparisons of our nonrelativistic electrostatic correlation energies and the RMBPT results for the $2s$-$2p$ and $2p_{1/2}$-$2p_{3/2}$ differences are presented in Figs. 2–4. The deviation between the two calculations at low Z comes from imprecision in the $\Delta E_{n\geq 1}$ coefficients [Eq. (2)] from our MCHF method. This effect decreases like $1/Z$ and becomes negligible for heavy ions. The relativistic contributions to electrostatic correlation are in good agreement between the two methods, except for the transition $2p_{1/2}$-$2s_{1/2}$ in uranium. The expected behavior for the relativistic contribution to the electrostatic correlation energy is Z^2. Our MCDF results for the transition $2p_{1/2}$-$2S_{1/2}$ behaves exactly as expected, while results from Ref. 7 do not. This could be due to higher-order effects not included in our calculation, or to numerical inaccuracy in the RMBPT calculation at high Z.

Finally, we have plotted in Fig. 7 the differences between the total energies from the two calculations. These differences are easily traced from differences in Breit correlations: The MCDF calculation does not include terms corresponding to the exchange of several, instantaneous transverse photons in the ladder approximation, while the RMBPT calculation includes those terms to third order (i.e., up to three exchanged photons). Both calculations lacks "box diagrams" contributions, where one photon line crosses the others (in the ladder approximation all photon lines are parallel). The second-order box diagram is expected to be of the order of few 0.1 eV. As experimental results with accuracies of 0.1 eV are now available,[34] the calculation of those terms becomes a great challenge. It also becomes important to go beyond the ladder approximation to match such experimental accuracies. At that level of accuracy, nuclear structure also become an issue. For very heavy elements the nuclear-size correction has to be included very carefully. We have recomputed our uranium transition energies with a more realistic nuclear model. Following Blundell, John-

TABLE VIII. Transition energies in lithiumlike uranium using deformed charge distribution (Ref. 36). Main contributions (eV) are the following: Coulomb, which includes mass polarization and Coulomb correlation energy; Breit, which is the sum of the magnetic, retarded, and magnetic correlation energies; and QED, which is the sum of one-particle self-energy, self-energy screening, and the three contributions to vacuum polarization. The nuclear polarization for the $2s$ is estimated as $\frac{1}{8}$ of the $1s$ value from Plunien *et al.* (Ref. 37).

Transition	Coulomb with correlations	Breit	QED	Nuclear polarization	Total (this work)	Total (Ref. 35)
$2p_{1/2}-2s$	286.038	36.756	-41.100	-0.126	281.6±0.9	281.023±0.6
$2p_{3/2}-2s$	4514.730	-16.192	-38.662	-0.126	4459.8	4459.38
$2p_{3/2}-2p_{1/2}$	4228.692	-52.948	2.438	0.000	4178.2	4178.36

son, and Sapirstein,[35] we have used a deformed Fermi change distribution for the ^{238}U nucleus. The parameters of this distribution have been measured very accurately by studying muonic x-rays for uranium.[36] Since the ground state of ^{238}U has $J=0$, we take the spherical average of the charge distribution. We also include approximate nuclear polarization correction to the self-energy.[37] Those results are presented in Table VIII. Error estimates in Table VIII take into account neither the missing box diagram contributions nor the uncertainties in the nuclear polarization.

IV. COMPARISONS WITH EXPERIMENT

It is impossible to compare directly the RMBPT results of Ref. 7 with experiment since they do not include radiative corrections. We have then arbitrarily decided to add to them hydrogenic radiative corrections and screening corrections estimated in Sec. II C. Another possible choice would have been to not include the screening corrections. Still this would have prevented a meaningful comparison, giving a difference between theory and experiment about 10 times larger than when the screening correction is included. This is a good hint that our method of approximation provides a good estimate of this screening correction in the low- to medium-Z range. For this comparison we have used recent data from Tokamak experiments[38-40] for $22 \leq Z \leq 42$. The $2p_{1/2}$-$2s$ and $2p_{3/2}$-$2s$ transition energies in xenon have been obtained in a beam-foil spectroscopy experiment at GANIL (France).[41] We have also included the recently published preliminary value for the $2p_{1/2}$-$2s$ transition energy in uranium.[34] Comparison between theory and experiment for the $2p_{1/2}$-$2s$ transition is shown in Fig. 8. Both calculations agree very well with experiment, with possible discrepancies less than 2×10^{-6} Z^3 eV up to $Z=54$ for the MCDF calculation. The $2p_{3/2}$-$2s$ transition energy (Fig. 9) and the $2p_{3/2}$-$2p_{1/2}$ energy separations (Fig. 10) are also very well represented by both theoretical predictions. The $2p_{3/2}$-$2p_{1/2}$ separation for $Z=54$ has also been measured at GANIL by comparing several $n=3$ to $n=2$ transitions observed with an x-ray spectrometer.[42]

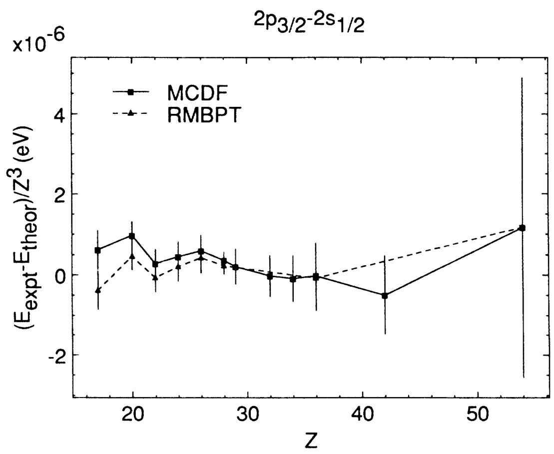

FIG. 9. Comparison between theory and experiment for $2p_{3/2}$-$2s$ transition. Error bars represent experimental contributions only.

From all three figures it is obvious that the RMBPT provide a better description of the low-Z behavior, because of the higher precision in the calculation of the nonrelativistic part of the electrostatic correlation. The difference is consistent with the error estimate presented in Sec. II E. The three figures also show that our method for evaluating radiative corrections is efficient and does not lead to errors much larger than the present experimental uncertainties. The fluctuations of the data around the theoretical values correspond to experimental irregularities larger than the published uncertainties.

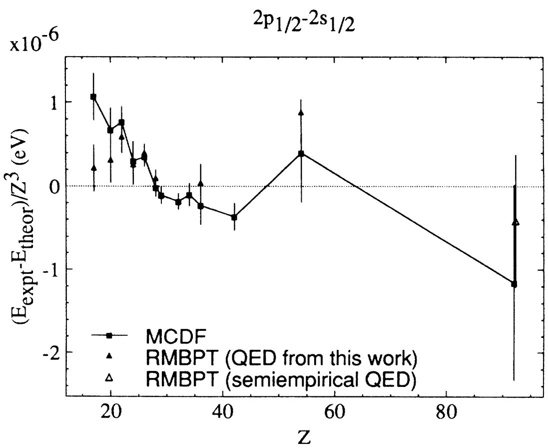

FIG. 8. Comparison between theory and experiment for $2p_{1/2}$-$2s$ transition. For $Z=92$ error bars represent quadratic combination of experimental and theoretical error bars. The RMBPT value is from Ref. 35. For all other elements error bars represent experimental contributions only.

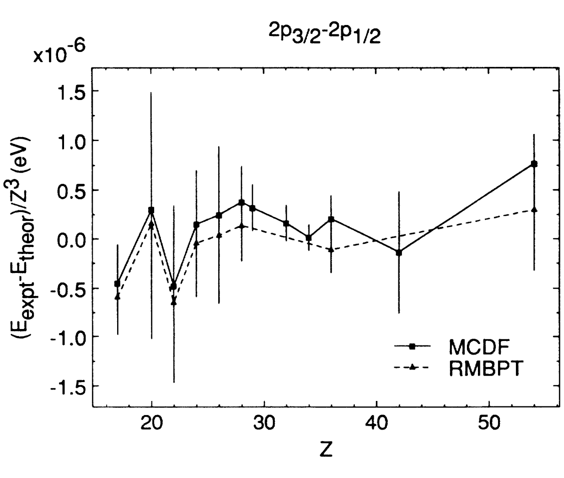

FIG. 10. Comparison between theory and experiment for $2p_{3/2}$-$2p_{1/2}$ splitting. Error bars represent experimental contributions only.

V. CONCLUSION

In this paper we have presented in detail theoretical transition energies in three-electron ions computed using the MCDF method. We have shown that, although many-electron QED corrections are still far from being computed from first principles, both MCDF and RMBPT methods (if corrected the self-energy screening with the approximation we have used), which are completely *ab initio,* can reproduce well all experimental data. In this respect both methods are very successful. The slightly better agreement of the RMBPT value (with semiempirical screening correction) with the recent $2p_{1/2}$-$2s$ experimental transition energy in uranium[34] is due to the better treatment of the magnetic correlation by that method compared to the present MCDF result.

The MCDF method usually provides easily 85% of the correlation energy. Beyond that, although one can reach in principle any precision by extending the basis set enough, it may be so cumbersome to do in practice (convergence problems, excessive computer time, etc.) that one has to stop below the precision one is hoping to get. This method also lacks a true many-body expression for the retarded part of the electron-electron interaction. To have more precise values for heavy elements it would be interesting to redo the MCDF calculations, including the magnetic interaction in the self-consistent-field process. Numerical problems have prevented us from doing so for large enough basis sets.

ACKNOWLEDGMENTS

We thank Dr. R. D. Deslattes and Dr. Y.-K. Kim for many helpful discussions, and Dr. W. C. Martin and A. W. Weiss for their suggestions for the improvement of this manuscript. We are much indebted to Professor W. R. Johnson for a very helpful explanation of his work, for having provided single-configuration calculations for $Z=92$, to improve the comparison between his results and ours, and for having provided his code to compute the spherical average of a deformed charge distribution. The MCDF calculations presented in this work have been done using the computer facility at the National Institute of Standards and Technology (NIST). One of us (P.I.) is very grateful to the Direction du Secteur Mathématiques et Physique de Base of Centre National de la Recherche Scientifique (CNRS), and to Dr. R. D. Deslattes and Dr. H. P. Kelly for their support of his stay at NIST. The LPAN, Laboratoire de Physique Atomique et Nucléaire, Université Pierre et Marie Curie, is "Unité Associée au CNRS No. 771."

---

[1] G. W. F. Drake, Can. J. Phys. **66**, 586 (1988).

[2] O. Gorceix, P. Indelicato, and J. P. Desclaux, J. Phys. B **20**, 639 (1987).

[3] P. Indelicato, O. Gorceix, and J. P. Desclaux, J. Phys. B **20**, 651 (1987).

[4] P. Indelicato, J. Phys. (Paris) Colloq. **48**, C-9 (1987).

[5] P. Indelicato, Nucl. Instrum. Methods Phys. Res. B **31**, 14 (1988).

[6] W. R. Johnson, S. Blundell, and J. Sapirstein, Phys. Rev. A **37**, 307 (1988).

[7] W. R. Johnson, S. Blundell, and J. Sapirstein, Phys. Rev. A **37**, 2764 (1988).

[8] J. P. Desclaux, Comput. Phys. Commun. **9**, 31 (1975).

[9] I. P. Grant, Adv. Phys. **19**, 747 (1970).

[10] C. Froese-Fisher, *The Hartree-Fock Method for Atoms* (Wiley, New York, 1977).

[11] W. R. Johnson and G. Soff, At. Data Nucl. Data Tables **33**, 405 (1986).

[12] O. Gorceix and P. Indelicato, Phys. Rev. A **37**, 1087 (1988).

[13] S. Love, Ann. Phys. (N.Y.) **113**, 153 (1978).

[14] J. Sucher, J. Phys. B **21**, L585 (1988).

[15] I. Lindgren, J. Phys. B **23**, 1085 (1990).

[16] P. Indelicato, J. Phys. (Paris) Colloq. **50**, C-1 239 (1989).

[17] D. S. Hughes and C. Eckart, Phys. Rev. **36**, 694 (1930).

[18] E. R. Cohen and B. N. Taylor, Rev. Mod. Phys. **59**, 1121 (1987).

[19] K. N. Huang, Y.-K. Kim, K. T. Cheung, and J. P. Desclaux, Phys. Rev. Lett. **48**, 1245 (1982).

[20] D. Layzer and J. Bahcall, Ann. Phys. (N.Y.) **7**, 177 (1962).

[21] Z. J. Horak, M. N. Lewis, A. Dalgarno, and P. Blanchard, Phys. Rev. **185**, 21 (1969).

[22] M. H. Mittleman, Phys. Rev. A **24**, 1167 (1981).

[23] I. P. Grant and H. M. Quiney, Adv. At. Mol. Phys. (to be published).

[24] L. W. Fullerton and G. A. Rinker, Phys. Rev. A **13**, 1283 (1976).

[25] P. J. Mohr, Ann. Phys. (N.Y.) **88**, 26 (1974).

[26] P. J. Mohr, Ann. Phys. (N.Y.) **88**, 52 (1974).

[27] P. J. Mohr, Phys. Rev. A **26**, 2338 (1982).

[28] J. Dupont-Roc, C. Fabre, and C. Cohen-Tannoudji, J. Phys. B **11**, 563 (1977).

[29] G. Feldman and T. Fulton, Ann. Phys. (N.Y.) **184**, 231 (1988).

[30] E. H. Wichmann and N. M. Kroll, Phys. Rev. **101**, 843 (1956).

[31] T. Beier and G. Soff, Z. Phys. D **8**, 129 (1988).

[32] F. A. Parpia and I. P. Grant, J. Phys. B **23**, 211 (1990).

[33] I. Lindgren, Phys. Rev. A **31**, 1273 (1985).

[34] J. Schweppe, A. Belkacem, L. Blumenfeld, N. Claytor, B. Feynberg, H. Gould, V. Kostroun, L. Levy, S. Misawa, R. Mowat, and M. Prior, Bull. Am. Phys. Soc. **35**, 1178 (1990).

[35] S. A. Blundell, W. R. Johnson, and J. Sapirstein, Phys. Rev. A **41**, 1698 (1990).

[36] J. Zumbro, E. B. Shera, Y. Tanaka, J. C. E. Bemis, R. A. Naumann, M. V. Hoehn, W. Reuter, and R. M. Steffen, Phys. Rev. Lett. **53**, 1888 (1984).

[37] G. Plunien, B. Müller, W. Greiner, and G. Soff, Phys. Rev. A **39**, 5428 (1989).

[38] B. Denne, G. Magyar, and J. Jacquinot, Phys. Rev. A **40**, 3702 (1989).

[39] B. Denne, E. Hinnov, J. Ramette, and B. Saoutic, Phys. Rev. A **40**, 1488 (1989).

[40] E. Hinnov, T. O. Team, B. Denne, and J. O. Team, Phys. Rev. A **40**, 4357 (1989).

[41] S. Martin, J. P. Buchet, M. C. Buchet-Poulizac, A. Denis, J. Desesquelles, M. Druetta, J. P. Grandin, D. Hennecart, X. Husson, and D. Leclerc, Europhys. Lett. **10**, 645 (1989).

[42] A. Simionovici, D. D. Dietrich, D. Leneman, and J. P. Grandin, Phys. Rev. A **41**, 5250 (1990).